AJNR

Intracranial cryptococcosis in immunocompromised patients: CT and MR findings in 29 cases.

R D Tien, P K Chu, J R Hesselink, A Duberg and C Wiley

AJNR Am J Neuroradiol 1991, 12 (2) 283-289
http://www.ajnr.org/content/12/2/283

Intracranial Cryptococcosis in Immunocompromised Patients: CT and MR Findings in 29 Cases

Robert D. Tien[1]
Pauline K. Chu[1]
John R. Hesselink[1]
Arthur Duberg[1]
Clayton Wiley[2]

CT and MR scans of 29 immunocompromised patients (28 with AIDS or ARC, one with diabetes mellitus) who had documented intracranial cryptococcal infection were reviewed retrospectively. All patients had CT studies; 26 received iodinated contrast agent. CT findings included normal results in nine of 29, atrophy only in 13 of 29, nonenhancing lesions in three of 29, enhancing lesions in two of 20, and foci of leptomeningeal calcification in two of 29. Ten patients had both CT and MR studies, and four received gadopentetate dimeglumine. Among these 10 patients, five had normal CT studies and one showed moderate central atrophy. All 10, however, had abnormal MR findings. We observed four patterns: (1) parenchymal cryptococcoma (3/10); (2) numerous clustered tiny foci that were hyperintense on T2-weighted images and nonenhancing on postcontrast T1-weighted images, located relatively symmetrically in the basal ganglia bilaterally and in midbrain, representing dilated Virchow-Robin spaces (4/10); (3) multiple miliary enhancing parenchymal and leptomeningeal nodules (1/10); and (4) a mixed pattern, consisting of dilated Virchow-Robin spaces with mixed lesions such as cryptococcoma and miliary nodules (2/10). In the group of six patients with dilated Virchow-Robin spaces (patterns 2 and 4), two received gadopentetate dimeglumine, but the Virchow-Robin space lesions did not enhance; among the remaining four patients, two received gadopentetate dimeglumine (one with pattern 1 and one with pattern 3) and the lesions did enhance. Three patients in our study subsequently died and autopsies were performed. The postmortem results revealed dilated Virchow-Robin spaces filled with fungi in the basal ganglia, which correlated well with MR findings.

The high frequency of invasion of the perivascular Virchow-Robin spaces by *Cryptococcus* detectable by MR is noteworthy, and we recommend this imaging technique when CNS cryptococcosis is suspected.

***ANJR* 12:283–289, March/April 1991; *AJR* 156: June 1991**

Cryptococcus neoformans is one of the most common infectious agents causing CNS infections in immunocompromised patients [1]. However, previous reports on the ability of CT to detect abnormalities have been disappointing [2, 3]. MR has proved to have higher sensitivity than CT for detecting many CNS abnormalities. This article describes the CT and MR imaging features of intracranial cryptococcosis with emphasis on MR imaging.

Materials and Methods

We studied 29 cases of CNS cryptococcal infection retrospectively from the records of our institution. In 19 patients only CT was performed; in 10 patients both CT and MR studies were obtained. Patients ranged in age from 19 to 57 years; all were men. Twenty-eight patients (97%) had AIDS or AIDS-related complex (ARC) and one had diabetes mellitus. Of the 28 patients with AIDS or ARC, 26 were homosexual and two were hemophiliacs who had contracted the disease through blood transfusions. In all cases, the CNS cryptococcosis was diagnosed by positive CSF antigen titer and culture.

Cranial CT studies had been done with a GE 9800 scanner for each patient at the time of

Received May 11, 1990; revision requested August 13, 1990; revision received September 12, 1990; accepted September 13, 1990.

[1] Department of Radiology, UCSD Medical Center, 225 Dickinson St., San Diego, CA 92103. Address reprint requests to R. D. Tien.

[2] Department of Pathology, UCSD Medical Center, San Diego, CA 92103.

0195-6108/91/1202-0283

initial presentation with CSF findings during admission. Twenty-six patients also had iodinated contrast studies. Five-millimeter-thick transaxial images were obtained through the brain. Ten patients also had MR studies on a 1.5-T GE Signa unit, and four patients received IV gadopentetate dimeglumine. In one patient (patient 29), a follow-up MR study was performed after antifungal treatment. MR studies generally were performed between 1 and 3 days after the CT scans were obtained. The CT and MR studies were reviewed and compared to look for distinctive features of cryptococcosis. Autopsies were conducted (between 4 and 7 days after imaging studies were performed) on the three patients who died, and postmortem results were correlated with the CT and MR studies.

Results

The CT and MR results are summarized in Table 1 and the CT findings are detailed in Table 2. Normal findings were seen in about one third of the patients (9/29) and various degrees of central or cortical atrophy only in about one half of the patients (13/29). Cerebral atrophy is a well-known feature of human immunodeficiency virus (HIV) infections involving the CNS [4] and was to be expected in view of our patient population (97% had AIDS or ARC). Three patients had nonenhancing small lesions in the brain (patients 18, 19, 24) and two patients had an enhancing lesion in the right frontal lobe (patients 20 and 25). Small foci of calcification in the leptomeningeal spaces and parenchyma were seen in two patients without an associated enhancing lesion (patients 17 and 22). These might represent the sequelae from a long-standing cryptococcal infection before admission to our hospital.

Among the 10 patients who also had MR studies, four received IV gadopentetate dimeglumine (Table 3). We observed four patterns of abnormal MR findings: (1) a parenchymal mass (cryptococcoma) in three patients (patients 20, 25, 28) (Fig. 1); (2) numerous tiny foci, which are hyperintense on T2-weighted images and nonenhancing on postcontrast T1-weighted images located relatively symmetrically in the basal ganglia bilaterally and also in the midbrain (which represent dilated Virchow-Robin spaces) in four patients (patients 21, 24, 26, 27) (Fig. 2); (3) multiple miliary enhancing parenchymal and leptomeningeal-cisternal nodules in one patient (patient 22) (Fig. 3); and (4) a mixed pattern, consisting of dilated Virchow-Robin spaces with mixed lesions such as cryptococcoma and miliary nodules in two patients (patients 23 and 29) (Figs. 4 and 5). In the group of six patients with dilated Virchow-Robin spaces (patterns 2 and 4), two patients received gadopentetate dimeglumine (patients 26 and 23). While the Virchow-Robin space lesions did not enhance, the other parenchymal and leptomeningeal lesions did show enhancement (patient 23). Two other patients received gadopentetate dimeglumine (patients 20 and 22), and their lesions enhanced. We found that among pattern 1 MR lesions (cryptococcoma) CT was able to demonstrate the two frontal lobe cases (patients 20 and 25), but missed a small lesion in midbrain owing to beam-hardening artifact (patient 28). In four cases of pattern 2 MR abnormalities (dilated Virchow-Robin space), CT studies missed three of them except the most severe instance (patient 24), which showed nonenhancing lucencies without mass effect in the basal ganglia bilaterally. In the patient with pattern 3 MR lesions (miliary enhancing nodules), CT scans showed foci of punctate calcification in the parenchyma and leptomeninges without enhancing lesions. The last two patients, who had pattern 4 MR lesions (mixed pattern), had CT scans that were unremarkable. One of these showed complete resolution of the lesions on a follow-up MR scan obtained after antifungal treatment (patient 29) (Fig. 5). Three patients in our study (patients 16, 24, 26) subsequently died, and autopsies were performed. The postmortem results in all three cases revealed dilated Virchow-Robin spaces filled with fungi in basal ganglia and small numbers of surrounding perivascular chronic inflammatory cells that consisted primarily of macrophages (Figs. 6 and 7). The pathologic findings correlated well with the presumptive dilated Virchow-Robin space lesions previously noted on MR (patients 24 and 26).

TABLE 1: CT and MR Findings in 29 Immunocompromised Patients with CNS Cryptococcosis

Patients	CT Findings	MR Findings
1–12	Atrophy	Not performed
13–16	Normal	Not performed
17	Punctate small foci of calcification	Not performed
18	Atrophy; nonenhancing lucency	Not performed
19	Atrophy; nonenhancing lucency	Not performed
20	Small enhancing nodule	Pattern 1
21	Atrophy	Pattern 2
22	Atrophy with punctate calcifications	Pattern 3
23	Normal	Pattern 4
24	Nonenhancing lucent foci	Pattern 2
25	Enhancing mass	Pattern 1
26	Normal	Pattern 2
27	Normal	Pattern 2
28	Normal	Pattern 1
29	Normal	First MR image = pattern 4; posttreatment image = normal

TABLE 2: CT Findings in 29 Immunocompromised Patients with CNS Cryptococcosis

CT Findings	No. of Patients
Normal	9
Atrophy	13
Nonenhancing lesions	3
Enhancing lesions	2
Foci of calcification	2

Discussion

Cryptococcus neoformans, the only *Cryptococcus* species known to be pathogenic in humans, can be isolated from soil contaminated by bird excreta. Most human infections are thought to be acquired through inhalation. Cryptococcosis is commonly associated with debilitating diseases, such as lymphoma, leukemia, multiple myeloma, sarcoidosis, tuberculosis, diabetes mellitus, and lupus erythematosus; it is also seen after glucocorticoid therapy. In the pre-AIDS era, up to 50% of patients in some reports had no form of immunodeficiency, but some impairment of lymphocyte response to cryptococci had been found in most cases [4]. By the time the diagnosis

of systemic cryptococcosis is established, 70% of patients have neurologic abnormalities [5].

Today, with the increase in AIDS cases, *Cryptococcus* ranks third after HIV and *Toxoplasma gondii* on the list of infectious agents causing CNS disease in AIDS [1]. Approximately 5% of AIDS patients develop CNS cryptococcosis [6]. The most common CNS infection caused by cryptococci is meningitis. The pathology ranges from mild congestion to meningeal thickening and distention of the subarachnoid space by abundant mucoid exudate. The characteristic absence of marked inflammatory reaction with only mild infiltration by lymphocytes and histiocytes is noteworthy.

The choroid plexus of the trigone is involved frequently, and spinal cord and spinal nerve roots may also be affected [7, 8]. Fungi may enter the Virchow-Robin space and give rise to small cysts (so-called "soap bubbles") or gelatinous pseudocysts in the parenchyma [9]. Deep gray matter structures, such as the basal ganglia, thalamus, and substantia nigra, may also contain multiple small cystic spaces; however, cerebral edema seldom occurs. In the immunologically intact host, these fungi usually induce a chronic granulomatous reaction.

In one review of the CT scans of 35 patients (among them 28 patients with AIDS) who had intracranial cryptococcal infection [2], the studies were found to be normal in 43%. Positive findings included diffuse atrophy in 34%, mass lesions (cryptococcoma) in 11%, hydrocephalus in 9%, and diffuse cerebral edema in 3%. One case of gelatinous pseudocysts of the basal ganglion and one case of intraventricular cryptococcal cyst were encountered. The diffuse atrophy pattern is most likely related to HIV infection rather than to fungal infection. The gelatinous pseudocysts were reported as nonenhancing cystic lesions of low density on contrast-enhanced CT [9] and of low signal intensity on T1-weighted MR images but high signal intensity—similar to CSF—on T2-weighted MR images [2].

TABLE 3: The Patterns of MR Findings in 10 Immunocompromised Patients with CNS Cryptococcosis

Pattern	No. of Patients	No. of Patients Who Received Gadopentetate Dimeglumine	MR Findings
1: Cryptococcoma: parenchymal mass	3	1	Mass enhanced with contrast
2: Dilated Virchow-Robin spaces	4	1	No evidence of enhancement
3: Miliary nodular lesions	1	1	Multiple enhancing nodules in the parenchyma and leptomeningeal spaces
4: Mixed pattern (pattern with mixed lesions such as patterns 1 and 3)	2	1	Dilated Virchow-Robin spaces did not enhance; other lesions enhanced

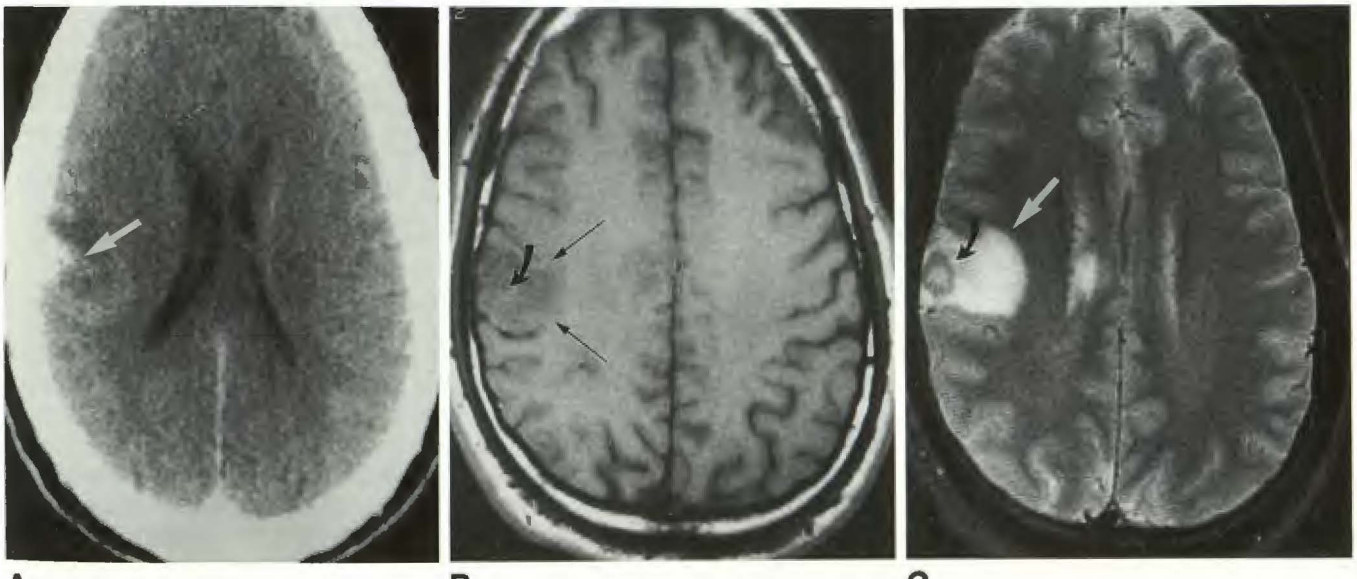

Fig. 1.—Pattern 1 (patient 25).

***A*, Contrast-enhanced CT scan shows small enhancing mass in right posterior frontal region abutting on skull with adjacent edema (*arrow*).**

***B*, Axial T1-weighted (600/20/2) MR image shows mass to be iso- to slightly hypointense relative to gray matter (*curved arrow*) with peripheral hypointensity representing edema (*straight arrows*).**

***C*, Axial T2-weighted (2500/80/2) MR image shows mass to be isointense with gray matter (*black arrow*), with a hyperintense center, perhaps representing central cystic-necrotic change. Peripheral edema is noted (*white arrow*).**

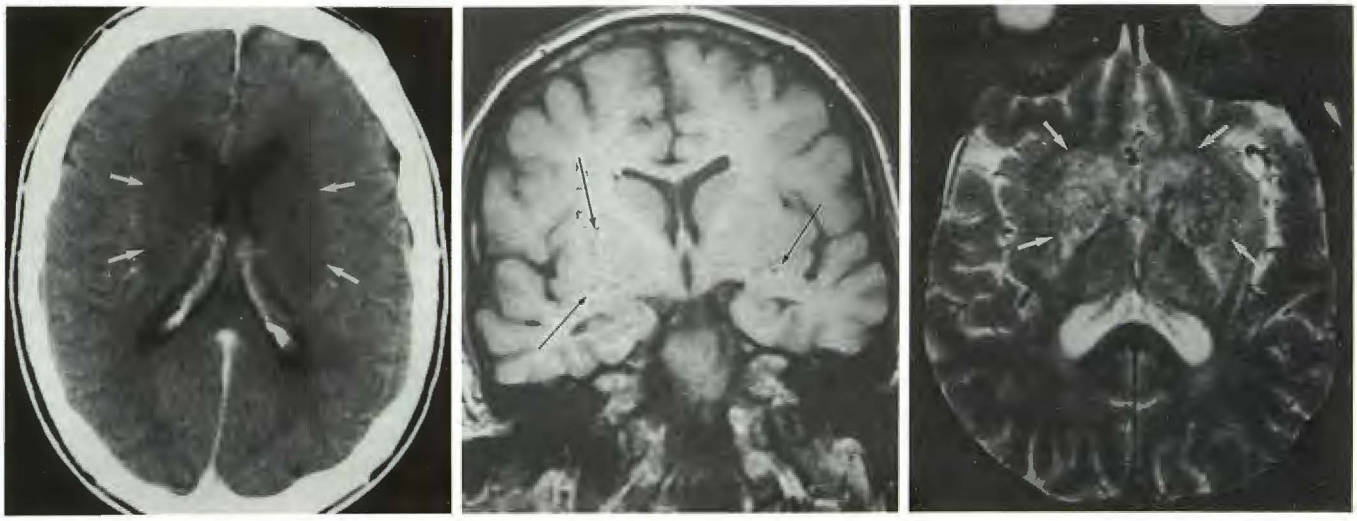

Fig. 2.—Pattern 2 (patient 24).
***A*, Contrast-enhanced CT scan shows nonenhancing lucencies in basal ganglia bilaterally without mass effect (*arrows*).**
***B*, Coronal T1-weighted (600/20) MR image shows multiple tiny hypointense foci in basal ganglia bilaterally (*arrows*). These represent dilated Virchow-Robin spaces.**
C, Axial T2-weighted (2500/80) MR image shows multiple clustered tiny hyperintense foci in basal ganglia bilaterally (*arrows*), which represent dilated Virchow-Robin spaces.

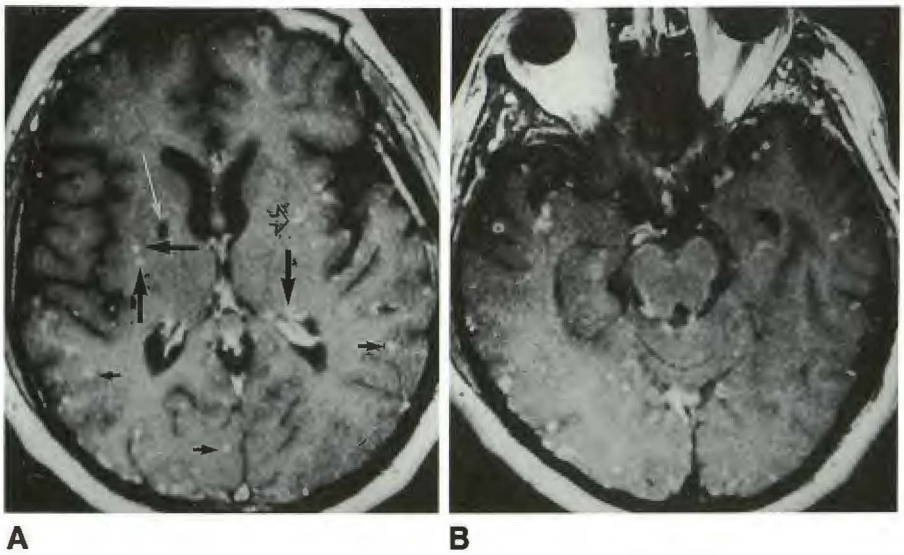

Fig. 3.—Pattern 3 (patient 22).
***A*, Postcontrast axial T1-weighted (600/20) MR image shows hypointense focus in right basal ganglia (large Virchow-Robin space, *long white arrow*). Hyperintense left putamen lesion noted on T2-weighted MR image (not shown) has enhanced (*open arrowhead*). Two enhancing nodules are noted in right external capsule, subependymal regions (*large black arrows*), and leptomeningeal-cisternal spaces (*small black arrows*), which cannot be seen on T2-weighted images.**
***B*, Postcontrast axial T1-weighted (600/20) MR image at a lower level shows multiple enhancing nodules in leptomeningeal-cisternal space.**

In another report of CT findings in 20 patients with CNS cryptococcal infection [3], only one patient was immunocompromised, secondary to systemic lupus erythematosus, and was treated with steroids and Cytoxan. Of these patients, 50% had normal CT scans, 25% had hydrocephalus, 15% had gyral enhancement, 15% had focal nodules, 10% had decreased white matter attenuation, and 5% had patchy uptake of contrast agent. The gyral enhancement, decreased white matter attenuation, and patchy uptake of contrast material are thought to represent various combinations of inflammation and pseudocyst formation in the meninges, perivascular Virchow-Robin space, and adjacent cerebral tissue [3]. The difference in the findings in these two reports is due to differences in the patient populations. The group with 28 AIDS patients revealed a high percentage of atrophy owing to HIV infection and a lower percentage of hydrocephalus [2]. Recently, Wehn and coworkers [10] reported two patients with AIDS complicated by cryptococcal meningitis who had focal hypodense, nonenhancing lesions on CT in the basal ganglia, with corresponding areas of increased T2 and decreased T1 signal on nonenhanced MR imaging. These lesions corresponded precisely to the distribution of the perforating arteries. The pathologic specimen showed these lesions to be small cystic collections of cryptococcal organisms in the dilated Virchow-Robin spaces with minimal inflammatory reaction. Balakrishnan et al. [11] also recently reported that the CNS cryptococcosis involvement of the basal ganglia in AIDS patients has a unique appearance on MR images,

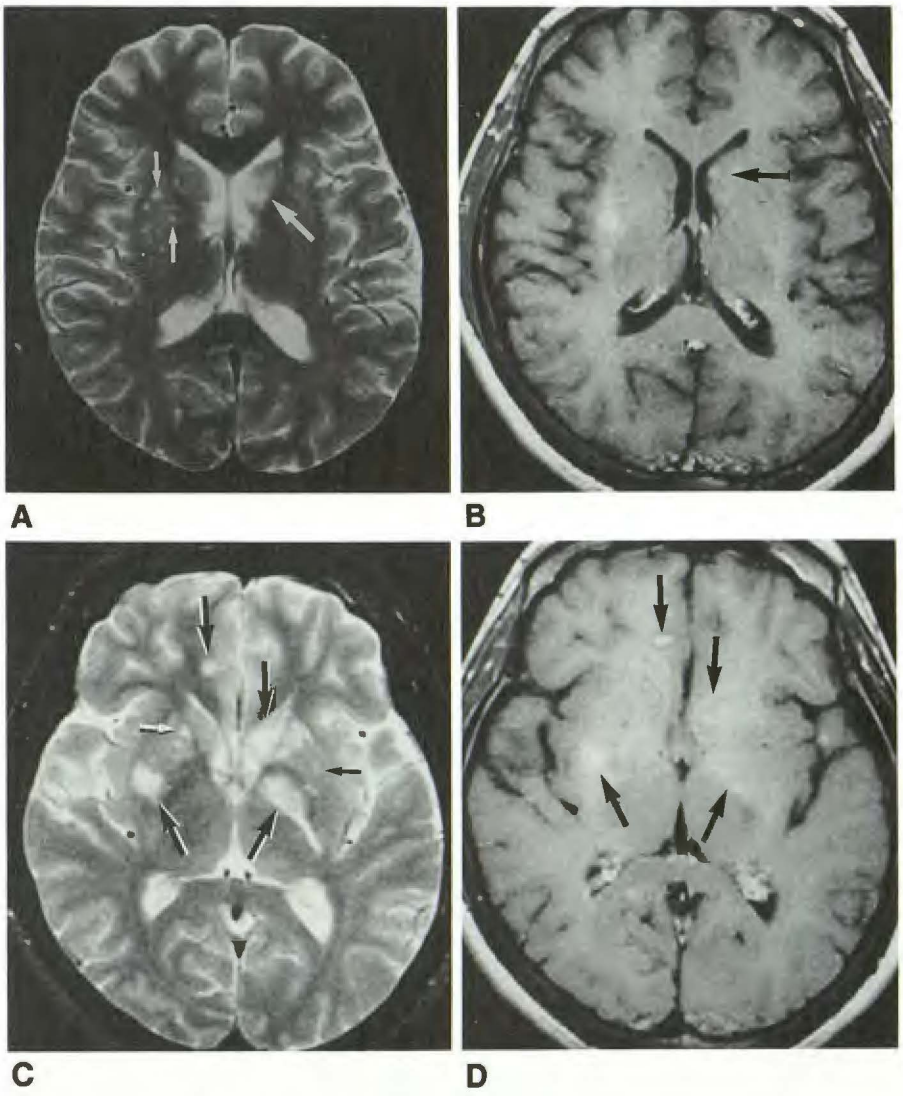

Fig. 4.—Pattern 4 (patient 23).

***A*, Axial T2-weighted (2500/80) MR image shows hyperintense lesion occupying left caudate nucleus (*large arrow*) and some smaller, clustered hyperintense lesions in right putamen (*small arrows*).**

***B*, Postcontrast axial T1-weighted (600/20) MR image at same level as in *A* shows irregular enhancement in left caudate nucleus (cryptococcoma) (*arrow*). However, the clustered right putamen lesions (dilated Virchow-Robin spaces) did not enhance.**

***C*, Axial T2-weighted (2500/80) MR image at a lower level shows varying irregularly sized hyperintense lesions in right putamen, left globus pallidus, left internal capsule posterior limb, left caudate nucleus, and right frontal lobe (*large arrows*). Small clustered hyperintense foci are present in anterior putamen regions bilaterally, representing dilated Virchow-Robin spaces (*small arrows*).**

***D*, Postcontrast T1-weighted (600/20) MR image at same level as in *A* shows enhancing lesions (*arrows*), which correlate well with irregular lesions seen on T2-weighted images. However, the clustered lesions seen on T2-weighted images (Virchow-Robin spaces) did not enhance.**

seen as bilateral, small, well-defined foci of high signal on T2-weighted images clustered in the basal ganglia. This appearance was not found with any of the other diseases, including toxoplasmosis, seen in their study.

The MR patterns of intracranial cryptococcosis in AIDS patients from our study (Table 3) included (1) cryptococcoma, (2) dilated Virchow-Robin spaces, (3) miliary enhancing nodules in the parenchyma and leptomeningeal-cisternal spaces, and (4) a mixed pattern. Pattern 1 (cryptococcoma) and pattern 3 (miliary nodules) are different presentations of hematogenous spread of the fungi. A breakdown occurs in the blood-brain barrier of the parenchymal lesions, and neovascular growth takes place around the leptomeningeal granulomas; hence, the lesions enhance with contrast agent. Although the leptomeningeal nodules are unremarkable on T2-weighted images, the postcontrast T1-weighted images can clearly demonstrate the lesions and are essential. As the vessels approach the CNS, they first course through the subarachnoid space and enter the cortex as thin-walled vessels. Between the vessel wall and the limiting glial membrane is the Virchow-Robin (perivascular) space. Normally this space gradually dwindles in size and ends as a fusion of perivascular and pial basement membranes. The space can be followed deep into the basal ganglia, white matter of the cerebellar peduncles, brainstem, and spinal cord. Near the termination of the space, the vessels become capillaries [12–15].

Heier et al. [16] found that slightly dilated Virchow-Robin spaces could be found in all age groups, probably as a normal condition. However, these researchers also noted that larger perivascular spaces are significantly associated with aging. In our patients, the dilated Virchow-Robin spaces were found in young patients who would not be expected to manifest this degree of dilatation under normal circumstances.

Jungreis et al. [17] pointed out that the greater sensitivity of MR imaging has allowed dilated perivascular spaces to be seen with greater frequency, and sometimes normal Virchow-Robin spaces have been mistaken for infarcts. Both these authors and others [16, 18] found that lesions in the lower one third of the putamen had the signal characteristics of CSF and were located in sites that corresponded to the distribution of the perforating arteries; these were thought to be dilated Virchow-Robin spaces. In contrast, lesions in the upper two

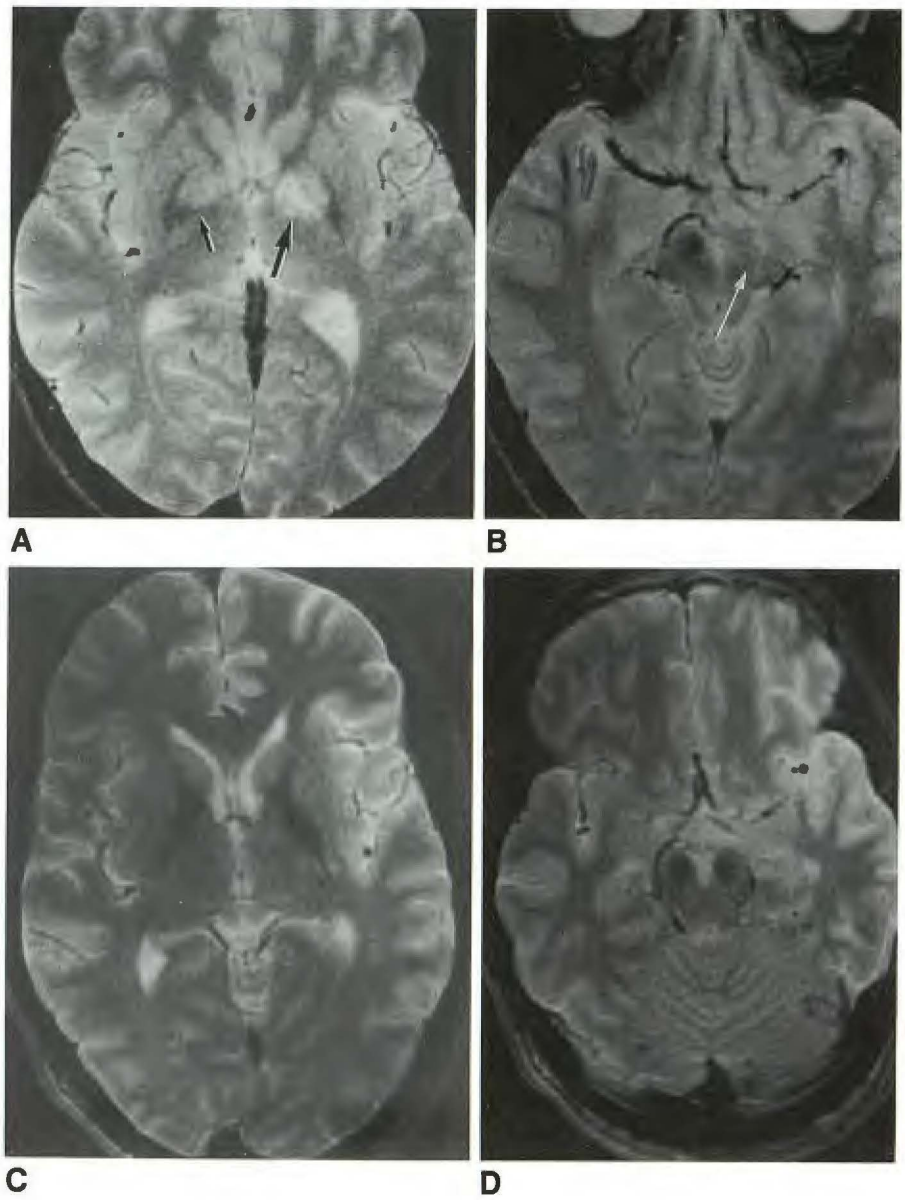

Fig. 5.—Pattern 4, pre- and posttreatment (patient 29).

A, Axial T2-weighted (2500/80) MR image shows clustered lesions in right basal ganglia (*small arrow*), which may represent dilated Virchow-Robin spaces. The left basal ganglia lesion (*large arrow*) is more confluent in shape and larger in size; this probably represents a cryptococcoma.

B, Axial T2-weighted (2500/80) MR image at midbrain level shows an enlarged left cerebral peduncular inhomogeneous hyperintense lesion (*arrow*) representing a cryptococcoma.

C and *D*, Axial T2-weighted (2500/80) MR images at same levels as in *A* and *B* after antifungal treatment show total resolution of lesions.

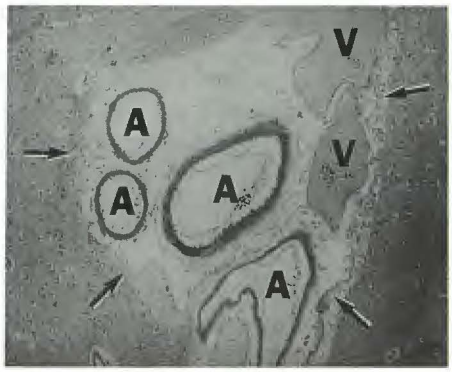

6

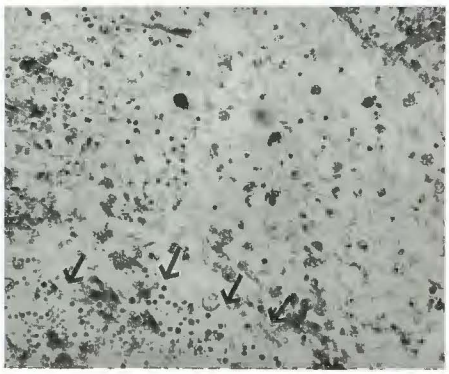

7

Fig. 6.—Paraffin section from the brain of patient 26. Several arteries (A) and veins (V) are noted within a dilated Virchow-Robin space (*arrows*) in the basal ganglia. (H and E ×40)

Fig. 7.—Within this dilated Virchow-Robin space of the basal ganglia, numerous lipid-filled macrophages surround a pocket (outlined by *arrows*) of darkly stained circular organism (*Cryptococcus neoformans*). (PAS ×160)

thirds of the putamen differed in signal characteristics and were presumed to represent lacunar infarction. However, in our patients, the lesions were all of identical intensity throughout the upper and lower basal ganglia regions, having the same signal intensity as CSF. In addition, the areas of high signal intensity appeared to be more numerous, with some even showing confluence, which correlated well with the histologic findings.

Fungal invasion of the perivascular spaces has been described in the literature [19, 20]. Dilated Virchow-Robin spaces filled with fungi are relatively isointense to slightly hypointense relative to gray matter on T1-weighted images, slightly hyperintense on proton-density-weighted images, and hyperintense on T2-weighted images (i.e., with the same signal intensity as CSF). They usually occur symmetrically in both upper and lower basal ganglia and are round or oval. Because the blood-brain barrier remains intact, no contrast enhancement is seen on either CT or MR studies (pattern 2). As the fungi invade the brain parenchyma and are not confined in the Virchow-Robin spaces, they can become confluent and patchy in appearance on T2-weighted images and enhance after contrast administration (pattern 4). In addition, some edematous changes may involve the internal capsule and track along the corticospinal tracts into the midbrain and pons. Nevertheless, the pattern 2 MR appearance (bilateral, numerous, small, well-defined foci of high signal on T2-weighted images and nonenhancing with contrast agent) is suggestive of CNS cryptococcosis but not pathognomonic, as we have seen one AIDS patient with CNS coccidioidomycosis documented by CSF culture and another patient with leukemia and systemic candidiasis whose MR study was very similar in appearance. Patterns 1 and 3 can be seen in various neoplastic and granulomatous diseases, and pattern 4 is the mixed pattern, which is nonspecific. In AIDS or ARC patients with lesions in the basal ganglia, toxoplasmosis and lymphoma should always be considered; however, these lesions usually show contrast enhancement and edema. The classic finding of hydrocephalus was not commonly seen in immunocompromised patients in a previous report [2], which is in keeping with our findings. Also, no evidence of diffuse confluent basal cisternal-leptomeningeal enhancement, which is often present in bacterial and tuberculous meningitis, was seen in any of our cases. This most likely is attributable to the lack of inflammatory leptomeningeal reaction and adhesions within the cisternal spaces in the immunocompromised patients that normally cause hydrocephalus. In a series of 24 patients with HIV encephalitis confirmed at autopsy, 18 had radiologic evidence of atrophy [21]. Atrophy was identified in more than half the cases in our patient population (16/29), which most likely was the result of CNS HIV infection.

CT can diagnose intraparenchymal masses and can detect foci of calcification, indicating the chronicity of these fungal infections. However, routine CT usually does not reveal dilated Virchow-Robin spaces [16–18] in the basal ganglia, which were evident on CT in only one of the six patients (patient 24) with positive MR findings in our series. In addition, these spaces could not be identified in the lower midbrain and pons by CT owing to beam-hardening artifacts.

In conclusion, MR imaging provides valuable information about CNS abnormalities in cryptococcal infections in immunocompromised patients. Of note are the dilated, fungi-filled Virchow-Robin spaces in the basal ganglia and midbrain seen by MR in a high percentage of patients. Although these lesions are not pathognomonic, rapid recognition can be helpful in determining proper treatment.

ACKNOWLEDGMENT

The authors are grateful to Catherine Fix for excellent editorial suggestions.

REFERENCES

1. Gabuzda DH, Hirsch MS. Neurologic manifestations of infection with human immunodeficiency virus. Clinical features and pathogenesis. *Ann Intern Med* **1987**;107:383–391
2. Popovich MJ, Arthur RH, Helmer E. CT of intracranial cryptococcosis. *AJNR* **1990**;11:139–142
3. Tan CT, Kuan BB. Cryptococcus meningitis, clinical-CT scan considerations. *Neuroradiology* **1987**;29:43–46
4. Perfect JR, Durack DT, Gallis HA. Cryptococcemia. *Medicine* **1983**;62: 98–109
5. Rowland LP. *Merritt's textbook of neurology*, 8th ed. Philadelphia: Lea & Febiger, **1988**:146–148
6. Eng RHK, Bishburg E, Smith SM, Kapilo, R. Cryptococcol infections in patients with acquired immune deficiency syndrome. *Am J Med* **1986**;81:19–23
7. Weenink HR, Bruyn GW. Cryptococcus in the nervous system. In: Vincken PJ, Bruyn GW, eds. *Handbook of clinical neurology*, vol. 35. Amsterdam: North Holland, **1978**:459–502
8. Penar PL, Kim J, Chyatte D, et al. Intraventricular cryptococcal granuloma. Report of two cases. *J Neurosurg* **1988**;68:145–148
9. Garcia CA, Weisberg LA, Lacorte WSJ. Cryptococcal intracerebral mass lesion: CT-pathologic considerations. *Neurology* **1985**;35:731–734
10. Wehn SM, Heinz R, Burger PC, et al. Dilated Virchow-Robin spaces in cryptococcal meningitis associated with AIDS: CT and MR findings. *J Comput Assist Tomogr* **1989**;13:756–762
11. Balakrishnan J, Becker PS, Kumar AJ, Zinreich SJ, McArthur JC, Bryan RN. Acquired immunodeficiency syndrome: correlation of radiologic and pathologic findings in the brain. *RadioGraphics* **1990**;10:201–215
12. Mirfakhraee M, Crofford MJ, Guinto FC, et al. Virchow-Robin space: path of spread in neurosarcoidosis. *Radiology* **1986**;158:714–720
13. Patek PR. Perivascular spaces in mammalian brain. *Anat Rec* **1944**;88: 1–24
14. Nelson E, Blinzinger K, Hager H. Electron microscopic observations on the subarachnoid and perivascular spaces of the Syrian hamster brain. *Neurology* **1961**;11:285–295
15. Jones EG. On the mode of entry of blood vessels into the cerebral cortex. *J Anat* **1970**;106:507–520
16. Heier LA, Bauer CJ, Schwartz L, et al. Large Virchow-Robin spaces: MR-clinical correlation. *AJNR* **1989**;10:929–936
17. Jungreis CA, Kanal E, Hirsch WL, et al. Normal perivascular spaces mimicking lacunar infarction: MR imaging. *Radiology* **1988**;169:101–104
18. Braffman BH, Zimmerman RA, Trojanowski JQ, et al. Brain MR: pathologic correlation with gross and histopathology. 1. Lacunar infarction and Virchow-Robin spaces. *AJNR* **1988**;9:621–628, *AJR* **1988**;151:551–558
19. Fetter BF, Klintworth GK, Hendry WS. *Mycoses of the central nervous system.* Baltimore: Williams & Wilkins, **1967**:89–123
20. Minckler J. *Pathology of the nervous system*. New York: McGraw-Hill, **1968**:494–497
21. Chrysikopoulos HS, Press GA, Grafe MR, Hesselink JR, Wiley CA. Encephalitis caused by human immunodeficiency virus: CT and MR imaging manifestations with clinical and pathologic correlation. *Radiology* **1990**;175:185–191